ENGINEERING TRANSACTIONS • *Engng. Trans.* • **61**, 4, 289–300, 2013
Polish Academy of Sciences • Institute of Fundamental Technological Research (IPPT PAN)
National Engineering School of Metz (ENIM)

Mechanical Properties of AW8S-V Polyester Composite under Various Loading Conditions

Wojciech MOĆKO[1),2)], Tadeusz SZYMCZAK[2)]
Zbigniew L. KOWALEWSKI[1)]

[1)] *Institute of Fundamental Technological Research PAN*
Pawińskiego 5B, 02-106 Warszawa, Poland

[2)] *Motor Transport Institute*
Jagiellońska 80, 03-301 Warsaw, Poland
e-mail: wmocko@ippt.pan.pl

This article presents the results of an analysis of the mechanical properties of the AW8S-V polyester composite reinforced by a roving fabric under tensile loading. The stress-strain curves show an increase of the maximum stress and elastic modulus with increasing strain rate. By contrast, an increase of the temperature led to decrease of the maximum stress and elastic modulus. It is also shown that, failure mechanisms are dependent on the loading type. Shear cracks occurred in the specimens under quasi-static loading whereas composite layers damage was observed under dynamic loading. Temperature increase resulted to stronger fragmentation of the specimens.

Key words: polyester composite, Hopkinson bar, high strain rate, damage.

1. Introduction

Polyester composites are commonly used in many different branches of industry, including the naval, aeronautics, motor transport and energetics (wind farm), because of their excellent mechanical properties, low cost, ease of fabrication and good strength-to-weight ratio. Polyester composites are applied, for example, in energy-absorbing structures [1, 2] and ballistic shields [3, 4]. Both of these applications involve exposure to extreme loading and high strain levels, which may lead to material damage. Therefore, material characterisation over a wide range of strain rates and temperatures is required for the design of energy-absorbing and protective structures. Previous studies of polyester matrix composites have reported that the strain rate affects the elastic modulus and maximum stress of these composite materials [1, 5]. In addition, it has been

observed that changes in the strain rate affect the mechanism by which material damage occurs.

This study analyses the mechanical properties of the AW8S-V polyester matrix composite, developed by the Military Institute of Armour and Vehicle Technology and the Alter Company. It was originally designed for a lightweight armour used by soldiers and military vehicles. The polyester composite, in the form of 8-mm plate, was made of the resin ATLAC 580 ACT and reinforced by 15 layers of the single oriented roving fabric STR-003-500-110.

2. Composite behaviour under monotonic deformation at various tensile strain rates

The objective of this section is to report the results of tests performed to evaluate the mechanical parameters of the AW8S-V, i.e., Young's modulus, ultimate tensile stress and their variations as a function of the tensile strain rate. All tests were conducted at room temperature on a servo-hydraulic Instron testing machine using flat specimens with a gauge length and width equal to 80 mm and 16 mm, respectively. Three load-frame velocities of the testing machine were applied, and as a result, the following strain rates were obtained: 2.0×10^{-4} s^{-1}, 3.0×10^{-4} s^{-1} and 4.2×10^{-3} s^{-1}. The material deformation was measured by a clip-on knife edge extensometer with a gauge length of 80 mm. To identify any possible anisotropy of the composite, the specimens were cut out from the composite plate along three directions, i.e., 0°, 45°, and 90°, with respect to the symmetry axis.

Figure 1 presents the stress-strain characteristics obtained for each orientation considered. The figure illustrates differences in the tensile curves, and hence differences in such mechanical parameters as Young's modulus and ultimate tensile stress. For the 0° and 90° orientations, the stress-strain relationship was

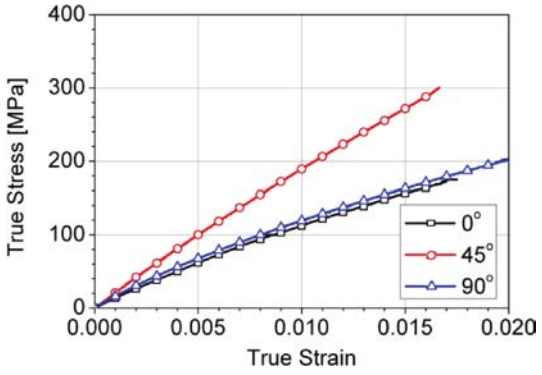

Fig. 1. Stress-strain characteristics of the composite, selected along the three directions considered.

non-linear, whereas for 45°, it could be well described by a linear function. The elastic modulus was strongly dependent on the specimens' orientation. For the directions indicated – 0°, 45° and 90° – the following values of the elastic modulus were obtained: 11890 MPa, 20186 MPa, 12902 MPa, respectively (Figs. 1 and 2a). The lowest ultimate tensile stress, 174 MPa, was recorded for the 0° orientation, whereas the highest, 301 MPa, was achieved for the 45° direction (Fig. 2b).

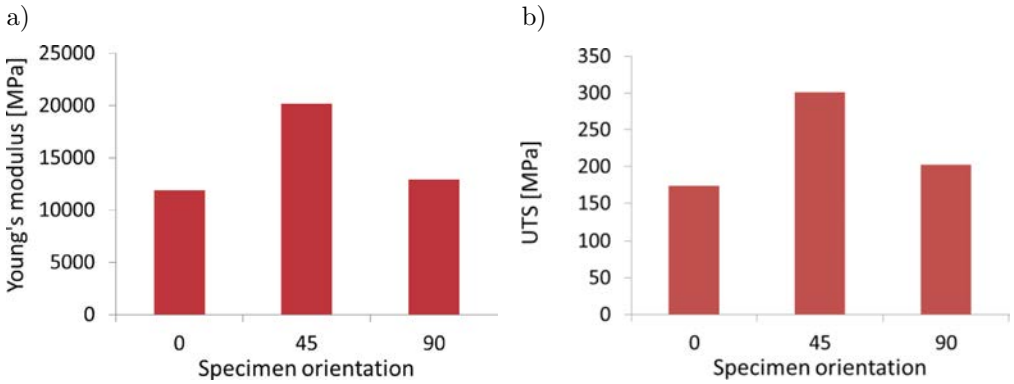

FIG. 2. Variations of Young's modulus (a) and ultimate tensile stress (b) *versus* specimen orientation.

In addition to the variation of the composite properties, different types of decohesion were clearly observed (Fig. 3a). A fracture zone of specimens cut

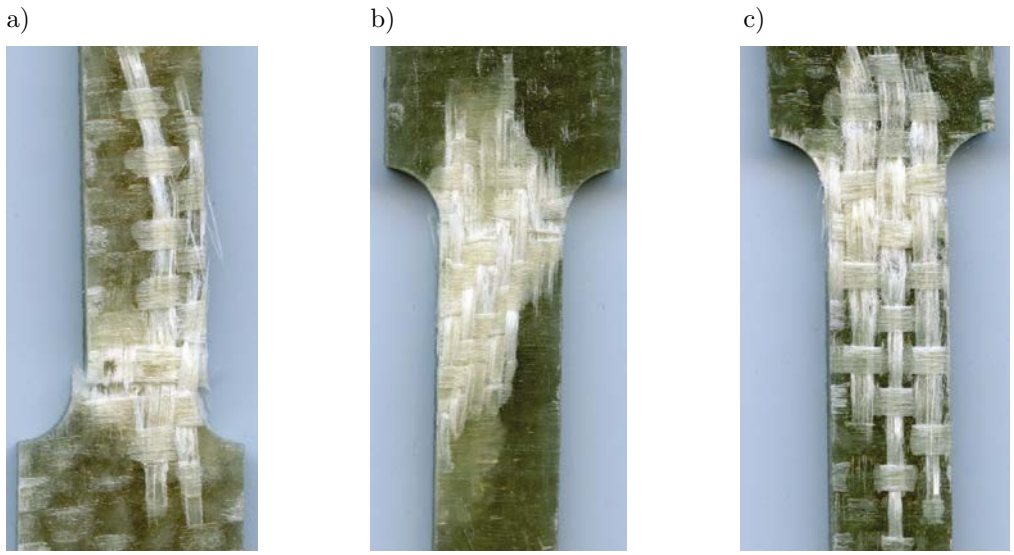

FIG. 3. Photographs of the fractured specimens cut out along the 0° (a), 45° (b) and 90° (c) directions.

out along the 0° and 90° directions showed similar features (Figs. 3a and 3c). Damage was developed mainly in the fibres oriented either longitudinal or perpendicular to the specimen surface. In the case of specimens cut out along the 45° direction, damage appeared over the whole cross-section of the material volume (Fig. 3b).

The effect of tension velocity on the mechanical parameters of the composite is illustrated in Fig. 4. It can be clearly observed that the Young's modulus and ultimate tensile stress for the 0° and 90° directions slightly increased in comparison to the their initial values. For specimens oriented along the 45° direction, a slight decrease of the Young's modulus and an increase of the ultimate tensile stress were obtained.

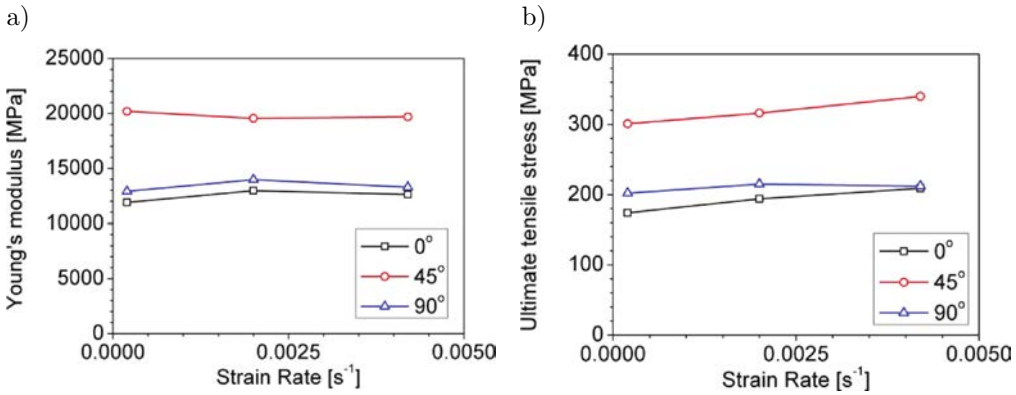

FIG. 4. Young's modulus (a) and ultimate tensile stress (b) *versus* strain rate.

3. Compression tests over wide range of strain rates and temperatures

An analysis of the mechanical properties of the polyester composite was performed using two different test setups for cylindrical specimens machined from the composite plate. The diameter and height of the specimens were equal to 8 mm. A servo-hydraulic testing machine equipped with a laser extensometer was used for the quasi-static deformation test, and the split Hopkinson pressure bar (SHPB) was applied for testing at high strain rates [6]. The SHPB test setup incorporated two bars of 2 m length and 20 mm diameter, which were fabricated using maraging steel characterised by a very high yield point (2200 MPa). Electrical signals measurements were carried using tensometers bonded to the centre of the bars. The electrical signals emitted by the tensometers were amplified using a wideband measurement bridge provided by Vishay, and the data were then captured and stored using an Agilent digital oscilloscope. The stress, strain and strain rate of the specimens were estimated based on the stress recorded in the

incident and transmitter bars, similarly to the method described in the literature [6–11]. Stress-strain curves of the AWS8S-V composite at various temperatures were obtained using the SHPB test setup equipped with an environmental chamber. To obtain a homogenous temperature distribution across the materials, the specimens were conditioned for 30 minutes before the start of mechanical testing. The subsequent deformation stages of the composite were recorded using a high-speed camera (Fig. 5).

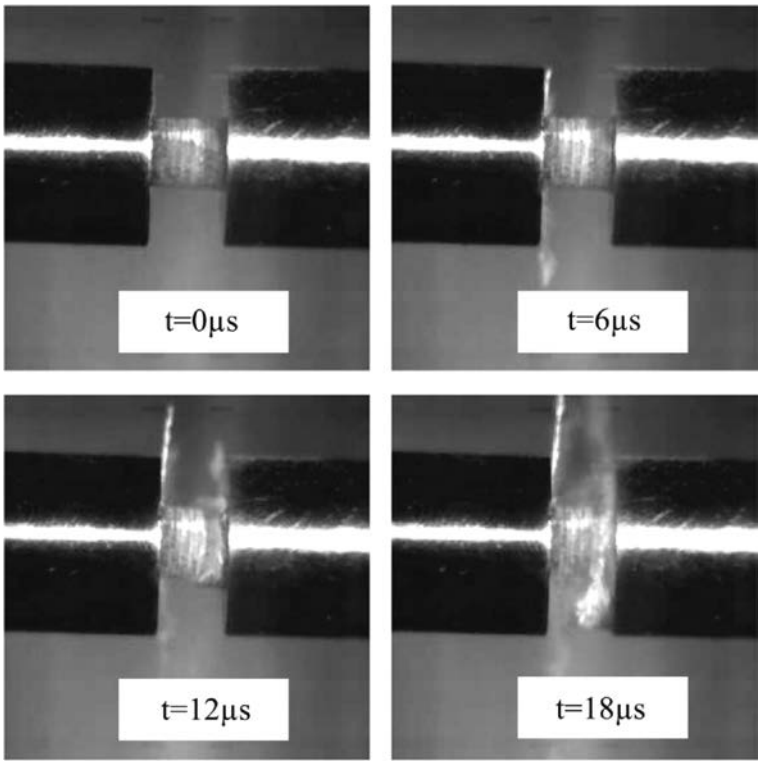

FIG. 5. Stages of composite compression using the SHPB method.

The results of the dynamic compression test, conducted over an initial temperature range of $-35°C$ to $100°C$, are shown in Fig. 6. Since the composite shows brittle behaviour it may be assumed that temperature increase due to plastic deformation is negligible. All stress-strain curves presented in this figure can be divided into three stages [12]. In the first stage, up to a strain $\varepsilon = 0.03$, a linear relationship between stress and strain was observed. At higher strain, all characteristics became non-linear, i.e., their slope with respect to the strain axis started to decrease. Such behaviour may be attributed to microdamage of the composite structure [13, 14]. In the final stage of deformation, macroscopic

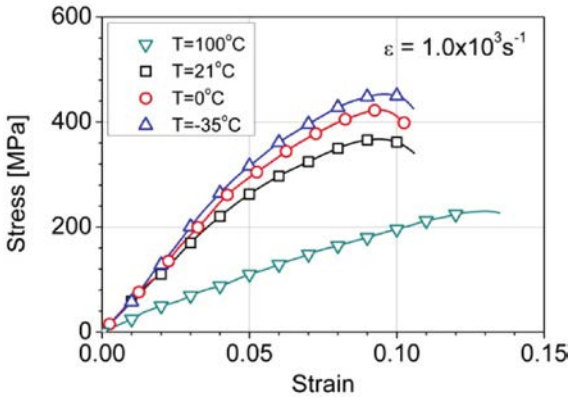

FIG. 6. Adiabatic stress-strain curves at various temperatures.

material damage appeared when the stress attained a maximum value, as shown in the diagram. Analysis of the curves shown in Fig. 6 indicates that the temperature increase led to a decrease of the stress-strain slope and the maximum stress required for macroscopic material damage to be initiated.

Photographs and SEM images of fractured specimens taken after the tests at various temperatures are shown in Fig. 7 and Fig. 8, respectively. The specimens tested at $-35°$C and $0°$C exhibited damage limited to a single composite layer of the material. The damage was manifested as extensive fragmentation of the composite without visible macroscopic cracks. Contrary to such behaviour, the specimens tested at higher temperatures, $21°$C and $100°$C, displayed strong fragmentation as well as delamination of the matrix and reinforcement phase.

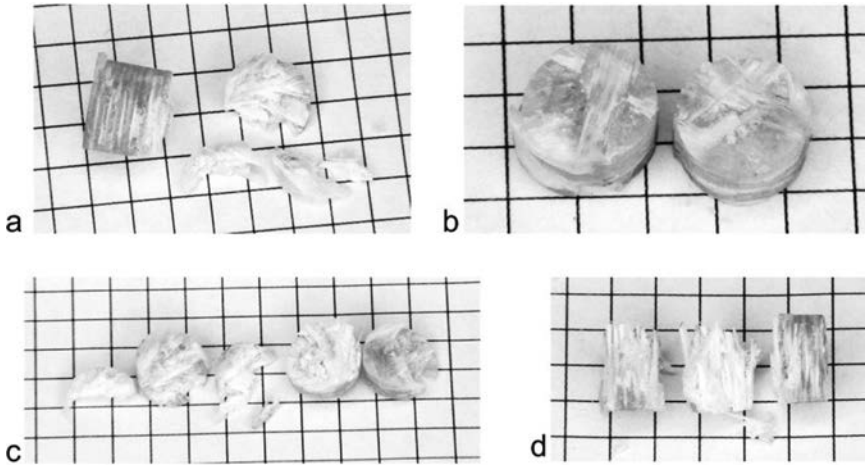

FIG. 7. Photographs of specimens damaged during dynamic loading at various temperatures: a) $T = -35°$C; b) $T = 0°$C; c) $T = 21°$C; d) $T = 100°$C.

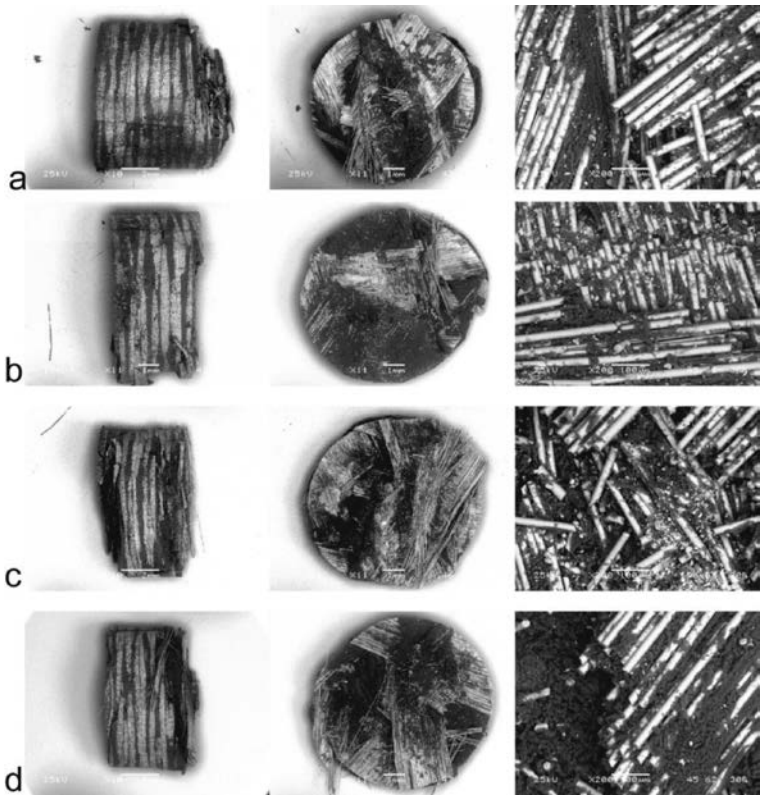

FIG. 8. SEM images of specimen damaged under dynamic loading conditions at various temperatures: a) $T = -35°C$; b) $T = 0°C$; c) $T = 21°C$; d) $T = 100°C$.

The stress-strain relationship calculated for various strain rates within the range of 1.9×10^{-4} s^{-1} to 1.6×10^{3} s^{-1} are shown in Fig. 9. An increase of the curves slope was observed with an increase of the strain rate.

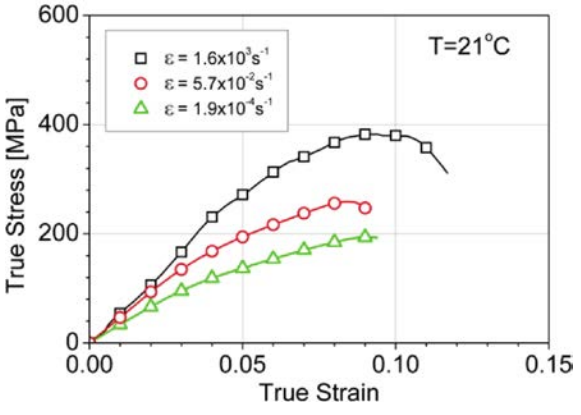

FIG. 9. Stress-strain curves at various strain rates.

Material damage occurred at the same strain level of approximately 0.08, independently of the strain rate, in all specimens tested. The maximum stress required for material damage increased significantly with the strain rate.

Photographs and SEM views of the specimens after compressive load testing at various strain rates are shown in Figs. 10 and 11, respectively. Oblique cracks

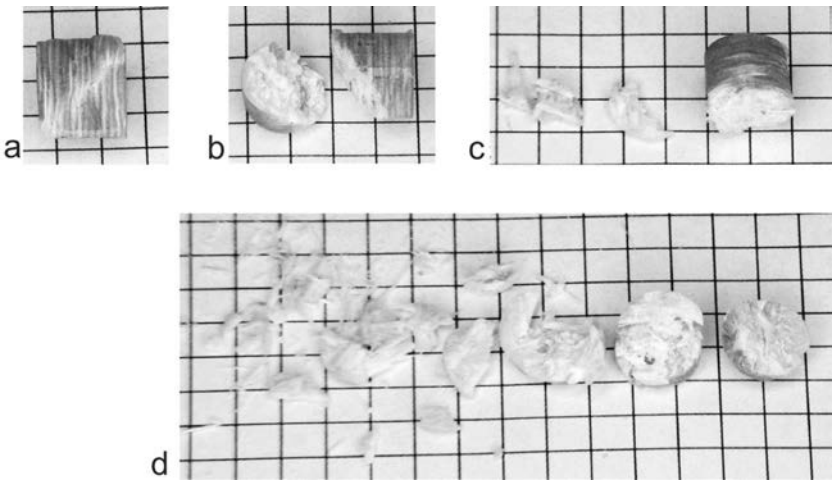

FIG. 10. Photographs of the specimens damaged at room temperature at various strain rates: a) $\dot{\varepsilon} = 1.9 \times 10^{-4}$ s^{-1}; b) $\dot{\varepsilon} = 5.7 \times 10^{-2}$ s^{-1}; c) $\dot{\varepsilon} = 1.0 \times 10^{3}$ s^{-1}; d) $\dot{\varepsilon} = 1.6 \times 10^{3}$ s^{-1}.

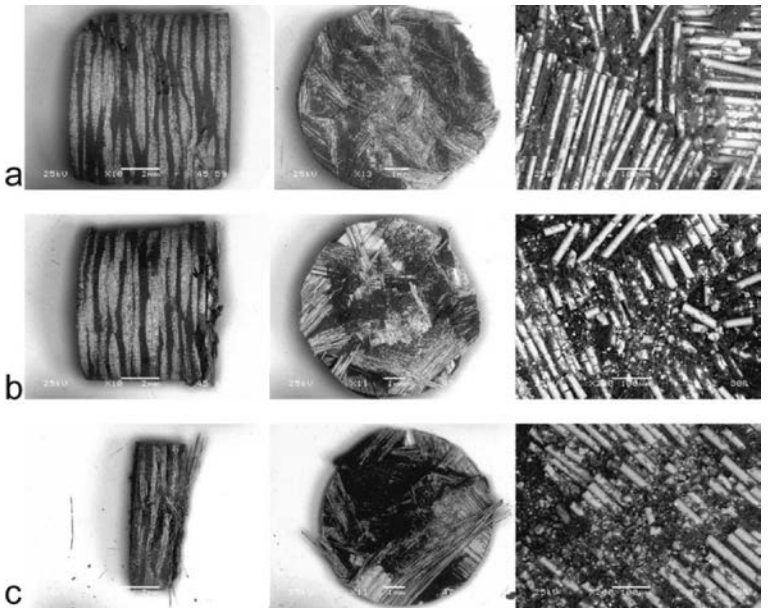

FIG. 11. SEM images of specimens damaged under dynamic loading conditions at various strain rates: a) $\dot{\varepsilon} = 5.7 \times 10^{-2}$ s^{-1}; b) $\dot{\varepsilon} = 1.0 \times 10^{3}$ s^{-1}; c) $\dot{\varepsilon} = 1.6 \times 10^{3}$ s^{-1}.

at an angle of 45° relative to the perpendicular direction were observed in the specimens that were tested using the servo-hydraulic testing machine. Therefore, it may be concluded that material damage occurs as a result of shear stress. For the strain rate of $1.9\times10^{-4}\ \mathrm{s}^{-1}$, a clearly visible crack without material separation was observed in the specimen. In the case of specimen tested at the strain rate of $5.7\times10^{-2}\ \mathrm{s}^{-1}$ it was split into two parts. Macroscopic oblique cracks were not visible in the specimens under dynamic loading, indicating that the mechanism of material damage is different than for the static one. At a strain rate of $1.0\times10^{3}\ \mathrm{s}^{-1}$, the surface layer of the composite was destroyed, whereas the further increase of the strain rate, up to $1.6\times10^{3}\ \mathrm{s}^{-1}$, resulted to the damage and fragmentation of the entire volume of the specimen.

The elastic modulus values were determined from the linear sections of the stress-strain curves and were observed to be strongly related to the temperature and strain rate, as shown in Fig. 12. It can be observed that the elastic modulus increased with the strain rate (Fig. 12a) due to the viscoelastic behaviour of the matrix material.

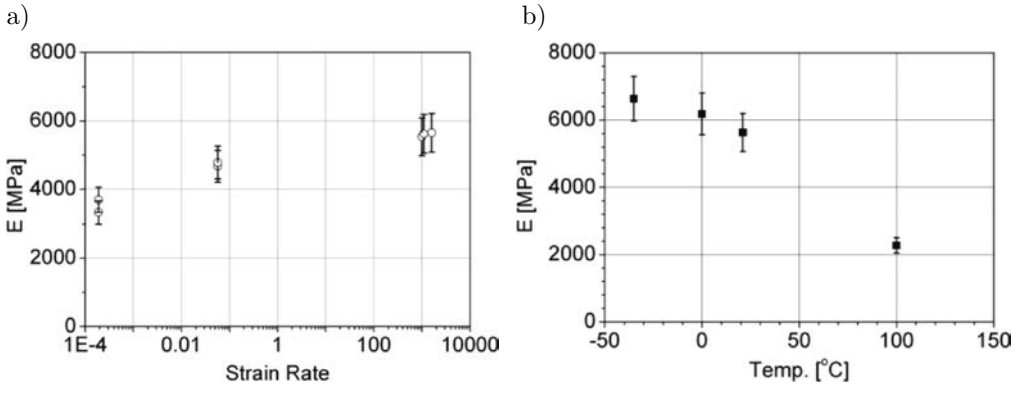

FIG. 12. Elastic modulus *versus* strain rate (a) and temperature (b).

Wide range of the mathematical models of mechanical behaviour of composites was already introduced [15–21]. In this work very accurate solution is proposed taking into account temperature and strain rate effect. The effect of the strain rate on the material stiffness may be described using the following formula [22]:

$$E_{rt} = E_0\left(1 + C_i \ln\frac{\dot{\bar{\varepsilon}}}{\dot{\bar{\varepsilon}}_0}\right), \qquad i = 2, ..., 4, \tag{3.1}$$

where E_{rt} – the rate-dependent stiffness; E_0 – the stiffness determined from quasi-static tests at a strain rate equal to $\dot{\bar{\varepsilon}}_0$; C_2, C_3 and C_4 – the strain rate constants for the longitudinal, shear and transverse modules, respectively; $\dot{\bar{\varepsilon}}$ – the

current strain rate. Equation (3.1) was calibrated using the data obtained during through-thickness compression tests performed over a wide range of strain rates. The experimental and model-based Young's moduli are compared in Fig. 13a.

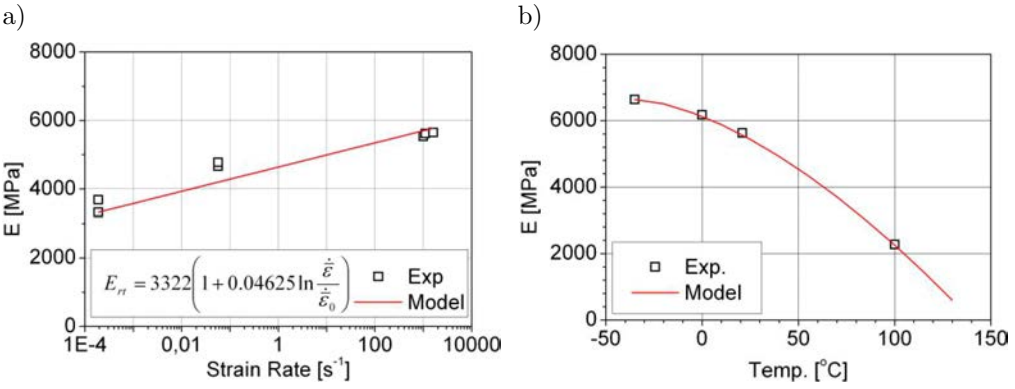

FIG. 13. Predictions of the elastic modulus versus strain rate (a) and temperature (b).

The other factor that affects the value of the elastic modulus is temperature. It can be observed that an increase of temperature causes material softening. The thermal softening phenomenon can be expressed analytically as follows:

$$E(T) = E_0\left[1 - \left(\frac{T - T_0}{T_m - T_0}\right)^m\right], \tag{3.2}$$

where E_0, T_m and m denote the Young's modulus at the reference temperature T_0, melting temperature, and temperature coefficient, respectively.

Taking into account Young's modulus dependence on both, strain rate and temperature, Eq. (3.1) and Eq. (3.2) can be rewritten as:

$$E(\dot{\varepsilon}, T) = E_0\left(1 + C_i \ln\frac{\dot{\varepsilon}}{\dot{\varepsilon}_0}\right)\left[1 - \left(\frac{T - T_0}{T_m - T_0}\right)^m\right], \qquad i = 2, ..., 4. \tag{3.3}$$

Based on experimental data obtained during Hopkinson bar tests at various temperatures, the following parameters were estimated: $E_0 = 46\,634$ MPa, $T_m = 140°$C and $m = 1.6$. The model prediction results are presented in Fig. 13b.

4. Conclusions

The mechanical properties of the polyester composite AWS8S-V were measured under tensile loading along three various directions of the composite sheet plane and under compressive loading perpendicular to the surface.

Summarising of the experimental results from tension tests, it is worth to emphasise that the AWS8S-V composite is an anisotropic material, and its mechanical properties are strongly dependent on the orientation of the material

volume. The maximum values of Young's modulus and ultimate tensile strength were achieved along the direction of 45°. As demonstrated by the results, these parameters were not significantly sensitive to variation of the tension velocity within the range of values applied.

The results of the compression test showed that the mechanical properties were strongly affected by the strain rate and temperature. Increase of the strain rate resulted in material hardening effects, including an increase of the elastic modulus and the generation of maximum stress leading to material damage [5, 23]. This behaviour may be caused by the viscoelastic properties of the composite matrix. In addition, the type of loading affects the mechanism of material damage; for example, shear cracks were observed under quasi-static loading conditions, whereas strong fragmentation of the material layers was observed under dynamic ones [23]. Rapid damage and delamination of the whole specimen volume occurred at the highest strain rate considered.

In addition, a temperature increase led to material softening behaviour, i.e. a decrease of the elastic modulus and generation of the maximum stress responsible for material damage. Stronger composite fragmentation and delamination were observed for higher values of temperature.

References

1. Solaimurugan S., Velmurugan R., *Progressive crushing of stitched glass/polyester composite cylindrical shells*, Compos. Sci. Technol., **67**, 422–437, 2007.
2. Obradovic J., Boria S., Belingardi G., *Lightweight design and crash analysis of composite frontal impact energy absorbing structures,* Compos. Struct., **94**, 423–430, 2012.
3. Almohandes A.A., Abdel-Kader M.S., Eleiche A.M., *Experimental investigation of the ballistic resistance of steel-fiberglass reinforced polyester laminated plates,* Compos. Part B-Eng., **27**, 447–458, 1996.
4. Buitrago B.L., García-Castillo S.K., Barbero E., *Experimental analysis of perforation of glass/polyester structures subjected to high-velocity impact*, Mater. Lett., **64**, 1052–1054, 2010.
5. Shah Khan M.Z., Simpson G., Townsend C.R., *A comparison of the mechanical properties in compression of two resin systems*, Mater. Lett., **52**, 173–179, 2002.
6. Kolsky H., *An Investigation of the mechanical properties of materials at very high rates of deformation of loading,* Proc. Phys. Soc., **62B**, 647, 1949.
7. Moćko W., Kowalewski Z.L., *Dynamic Compression Tests – Current Achievements and Future Development*, Eng. Trans., **59**, 235–248, 2011.
8. Moćko W., Kruszka L., *Results of Strain Rate and Temperature on Mechanical Properties of Selected Structural Steels*, Procedia Engineering, **57**, 789–797, 2013.
9. Moćko W., Kowalewski Z.L., *Application of FEM in the assessment of phenomena associated with dynamic investigations on a miniaturised DICT testing stand*, Kovove Mater., **51**, 71–82, 2013.

10. Moćko W., Rodríguez-Martínez J.A., Kowalewski Z.L., Rusinek A., *Compressive viscoplastic response of 6082-T6 and 7075-T6 aluminium alloys under wide range of strain rate at room temperature: Experiments and modelling,* Strain, **48**, 498–509, 2012.

11. Moćko W., Kowalewski Z.L., *Mechanical properties of the A359/SiCp metal matrix composite at wide range of strain rates*, Appl. Mech. Mater., **82**, 166–171, 2011.

12. Di Bella G., Calabrese L., Borsellino C., *Mechanical characterization of a glass/polyester sandwich structure for marine applications,* Mater. Design., **42**, 486–494, 2012.

13. Sumelka W., Łodygowski T., *The influence of the initial microdamage anisotropy on macrodamage mode during extremely fast thermomechanical processes*, Arch. Appl. Mech., **81**, 1973–1992, 2011.

14. Glema A., Łodygowski T., Sumelka W., Perzyna P., *The numerical analysis of the intrinsic anisotropic microdamage evolution in elasto-viscoplastic solids,* Int. J. Damage Mech., **18**, 205–231, 2009.

15. Gieleta R., Kruszka L., *Dynamic testing of reinforced glass fibre-epoxy composite at elevated temperatures*, Strength Mater., **34**, 238–241, 2002.

16. Mahmoudi N., Hebbar A., Zenasni R., Lousdad A., *Effect of impact directions, fiber orientation, and temperature on composite material*, J. Compos. Mater., **43**, 1713–1727, 2009.

17. Wang W., Makarov G., Shenoi R.A., *An analytical model for assessing strain rate sensitivity of unidirectional composite laminates*, Compos. Struct., **69**, 45–54, 2005.

18. Shokrieh M.M., Omidi M.J., *Compressive response of glass-fiber reinforced polymeric composites to increasing compressive strain rates*, Compos. Struct., **89**, 517–523, 2009.

19. Thiruppukuzhi S.V., Sun C.T., *Models for the strain-rate-dependent behaviour of polymer composites*, Compos. Sci. Technol., **61**, 1–12, 2001.

20. Thiruppukuzhi S.V., Sun C.T., *Testing and modelling high strain rate behaviour of polymeric composites*, Compos. Part B, **29B**, 535–546, 1998.

21. Xia Y., Wang X., *Constitutive equation for unidirectional composites under tensile impact*, Compos. Sci. Technol., **56**, 155–160, 1996.

22. Kara A., Tasdemirci A., Guden M., *Modeling quasi-static and high strain rate deformation and failure behaviour of a (±45)symmetric E-glass/polyester composite under compressive loading,* Mater. Design., **49**, 566–574, 2013.

23. Shah Khan M.Z., Simpson G., *Mechanical properties of a glass reinforced plastic naval composite material under increasing compressive strain rates,* Mater. Lett., **45**, 167–174, 2000.

Received August 27, 2013; revised version November 12, 2013.